

SIMULATION STUDY OF THE EFFECT OF IMPURITIES ON THE NONLINEAR DYNAMIC PROCESS OF EDGE-LOCALIZED-MODES

T.H. HUANG, T.Y. LIU, S.F. MAO, M.Y. YE

University of Science and Technology of China, Hefei, China

Email: sfmao@ustc.edu.cn; yemy@ustc.edu.cn

It is crucial to avoid large edge-localized modes (ELMs) to achieve high confinement steady plasma operation state. While the radiative impurities are necessary for achieving divertor detachment especially for the future tokamak [1], it is also found to have essential effects on ELM control [2]. Therefore, the mechanism how impurities affect the dynamic of ELMs is of great concern. Simulation studies based on “indirect” effects of impurities, such as radiative cooling, profile regulation and fuel dilution, have been considered in the linear instability analysis [3-5], which is insufficient to explain the complicated ELM behaviors observed in experiments [6, 7].

In this work, a systematical simulation study of the dynamical effect of impurities on pedestal stability, ELM evolution and turbulence transport is carried out. The simulations are performed using BOUT++ six-field two-fluid module [8], where the impurity model developed by Li et al. [9] (for studying the impurity dynamics in ELM-free QH-mode) is integrated. The simulations are implemented with self-consistent $n = 0$ electric field and parallel current evolution according to Seto et al.’s work [10, 11]. In addition, electron inertia is also considered for self-consistent current dissipation in fast magnetic reconnection.

The nonlinear simulation results of the ELM size based on EAST equilibrium (shot #91616, $t = 6$ s, ELM suppressed) are shown in Fig. 1. It can be seen that, ELM can be completely suppressed only when including the vorticity shear ϖ due to impurities, which reflects the essential role of impurity dynamics in ELM suppression.

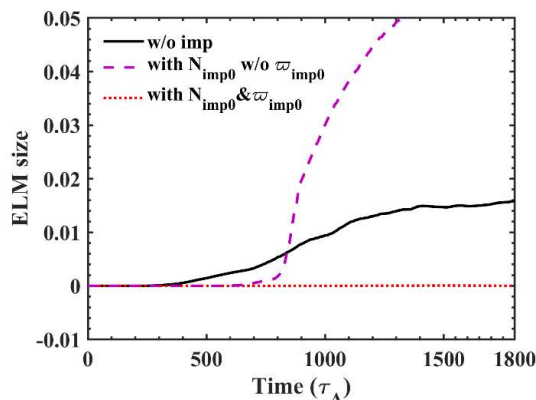


Figure 1. Time evolution of pedestal energy loss (ELM size) with different impurity effect: original model without impurity effect (solid black curve); only dilution effect of impurity considered (purple dashed curve); both dilution effect and vorticity shear due to impurities considered (dotted red curve).

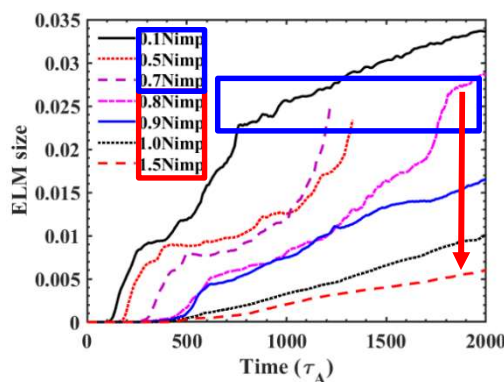


Figure 2. Time evolution of ELM size with different impurity densities. Ion and electron densities are varied accordingly to keep the same initial total pressure $P_0 = P_{i0} + P_{e0} + P_{imp0}$.

A scan of the impurity density is further performed. As shown in Fig. 2, when the multiplier of impurity density is below 0.7, the ELM size is large, while when the multiplier of impurity density is above 0.9, the ELM size is obviously reduced and the effect becomes significant with the increase of the multiplier. It implies that there is an impurity density “threshold” for ELM suppression, which is qualitatively consistent with experiment result in HL-2A [7].

The impurity effect on the ELM dynamic process is further explored in the $R_{imp} - (\text{pedestal}) T_e$ plane, where R_{imp} is the impurity density ratio defined as $m_{imp}n_{imp}/m_Dn_D$. As shown in Fig. 3, four regions can be identified in the $R_{imp} - T_e$ plane according to the difference of the “two-stage burst” [11] feature (see the pink curve for “0.8Nimp” in Fig. 2, where the first stage is at $\sim 600 \tau_A$ and the second at $\sim 1700 \tau_A$). It is found that the first stage is related to linear trigger of peeling-ballooning (P-B) mode and the second stage is nonlinear triggered due to the drift-tearing mode [12]. According to the shift of operation point among different regions, the different effect of impurity on the ELM evolution can be understood.

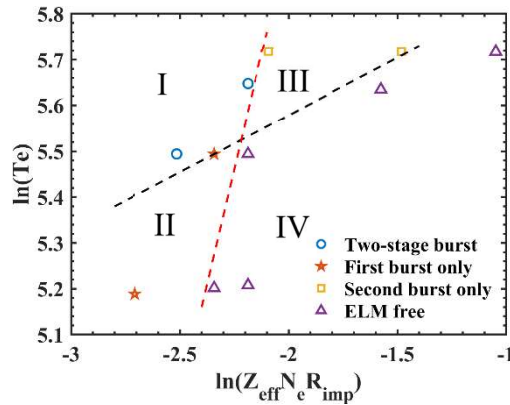


Figure 3. The $R_{imp} - T_e$ plane is divided into four regions by the stability boundaries of P-B mode (red dashed curve) and drift-tearing mode (black dashed curve). The feature of ELM dynamic process in the four regions are: I. Two-stage burst (blue circles); II. First burst only (red stars); III. Second burst only (yellow squares); IV. ELM free (purple triangles).

REFERENCES

- [1] A. W. Leonard, Plasma detachment in divertor tokamaks, Plasma Physics and Controlled Fusion (2018) 044001
- [2] G. S. Xu, Y. F. Wang, Q. Q. Yang, et al., Recent advances in developing natural and impurity-induced small/no-ELM H-mode regimes in EAST, Reviews of Modern Plasma Physics (2023) 14
- [3] H. Lan, T. H. Osborne, R. J. Groebner, et al., H-mode pedestal improvements with neon injection in DIII-D, Nuclear Fusion (2020) 056013
- [4] T. H. Osborne, G. L. Jackson, Z. Yan, et al., Enhanced H-mode pedestals with lithium injection in DIII-D, Nuclear Fusion (2015) 063018
- [5] J. Rapp, T. Eich, M. v. Hellermann, et al., ELM mitigation by nitrogen seeding in the JET gas box divertor, Plasma Physics and Controlled Fusion (2002) 639
- [6] X. Lin, G. S. Xu, Q. Q. Yang, et al., Physical mechanisms for the transition from type-III to large ELMs induced by impurity injection on EAST, Physics Letters A (2022) 127988
- [7] G. L. Xiao, X. L. Zou, W. L. Zhong, et al., Dual effects of impurity seeding on pedestal turbulence and ELMs in the HL-2A tokamak, Nuclear Fusion (2021) 116011
- [8] T. Y. Xia, X. Q. Xu and P. W. Xi, Six-field two-fluid simulations of peeling-ballooning modes using BOUT++, Nuclear Fusion (2013) 073009
- [9] Z. Li, X. Chen, C. M. Muscatello, et al., Numerical modeling of pedestal stability and broadband turbulence of wide-pedestal QH-mode plasmas on DIII-D, Nuclear Fusion (2022) 076033
- [10] H. Seto, X. Q. Xu, B. D. Dudson, et al., Interplay between fluctuation driven toroidal axisymmetric flows and resistive ballooning mode turbulence, Physics of Plasmas (2019)
- [11] H. Seto, X. Q. Xu, B. D. Dudson, et al., Two-stage crash process in resistive drift ballooning mode driven ELM crash, Physics of Plasmas (2024) 032513
- [12] A. B. Hassam, Fluid theory of tearing instabilities, The Physics of Fluids (1980) 2493-2497